AMERICAN SOCIETY FOR MICROBIOLOGY | Journal of Virology®

VIRUS-CELL INTERACTIONS

Phosphatidylethanolamine and Phosphatidylserine Synergize To Enhance GAS6/AXL-Mediated Virus Infection and Efferocytosis

Lizhou Zhang,[a] Audrey S. Richard,[a]* Cody B. Jackson,[a] Amrita Ojha,[a] Hyeryun Choe[a]

[a]Department of Immunology and Microbiology, The Scripps Research Institute, Jupiter, Florida, USA

Lizhou Zhang and Audrey S. Richard contributed equally to this work. Author order was determined based on the time spent on the project.

ABSTRACT Phosphatidylserine (PS) receptors mediate clearance of apoptotic cells—efferocytosis—by recognizing the PS exposed on those cells. They also mediate the entry of enveloped viruses by binding PS in the virion membrane. Here, we show that phosphatidylethanolamine (PE) synergizes with PS to enhance PS receptor-mediated efferocytosis and virus entry. The presence of PE on the same surface as PS dramatically enhances recognition of PS by PS-binding proteins such as GAS6, PROS, and TIM1. Liposomes containing both PE and PS bound to GAS6 and were engulfed by AXL-expressing cells much more efficiently than those containing PS alone. Further, infection of AXL-expressing cells by infectious Zika virus or Ebola, Chikungunya, or eastern equine encephalitis pseudoviruses was inhibited with greater efficiency by the liposomes containing both PS and PE compared to a mixture of liposomes separately composed of PS and PE. These data demonstrate that simultaneous recognition of PE and PS maximizes PS receptor-mediated virus entry and efferocytosis and underscore the important contribution of PE in these major biological processes.

IMPORTANCE Phosphatidylserine (PS) and phosphatidylethanolamine (PE) are usually sequestered to the inner leaflet of the plasma membrane of the healthy eukaryotic cells. During apoptosis, these phospholipids move to the cell's outer leaflet where they are recognized by so-called PS receptors on surveilling phagocytes. Several pathogenic families of enveloped viruses hijack these PS receptors to gain entry into their target cells. Here, we show that efficiency of these processes is enhanced, namely, PE synergizes with PS to promote PS receptor-mediated virus infection and clearance of apoptotic cells. These findings deepen our understanding of how these fundamental biological processes are executed.

KEYWORDS Chikungunya virus, Ebola virus, phosphatidylserine, Zika virus, eastern equine encephalitis virus, efferocytosis, liposome, phosphatidylethanolamine, synergy

Removal of apoptotic cells is central to the maintenance of healthy tissues. In healthy cells, phosphatidylserine (PS) is localized on the inner leaflet of the plasma membrane but externalized during apoptosis (1). Early in the apoptotic process, flippases that maintain membrane asymmetry are inactivated, and scramblases that dissipate phospholipid asymmetry are activated, and as a consequence, PS is redistributed to the cell surface. Externalized PS is recognized by PS receptors, whose major function is to recognize surface-exposed PS and induce efferocytosis, an immune-silent process by which phagocytes swiftly remove apoptotic bodies. These PS receptors also recognize PS on enveloped viruses and fortuitously support their entry into the target cells by mediating both attachment and internalization,

Citation Zhang L, Richard AS, Jackson CB, Ojha A, Choe H. 2021. Phosphatidylethanolamine and phosphatidylserine synergize to enhance GAS6/AXL-mediated virus infection and efferocytosis. J Virol 95:e02079-20. https://doi.org/10.1128/JVI.02079-20.

Editor Rebecca Ellis Dutch, University of Kentucky College of Medicine

Address correspondence to Hyeryun Choe, hchoe@scripps.edu.

* Present address: Audrey S. Richard, European Research Infrastructure on Highly Pathogenic Agents (ERINHA), Paris, France.

Received 22 October 2020
Accepted 23 October 2020
Accepted manuscript posted online 28 October 2020
Published 22 December 2020

a process described as "viral apoptotic mimicry" (2). Among these PS receptors, T-cell immunoglobulin mucin (TIM)- and TYRO3, AXL, and MERTK (TAM)-family members are best characterized for their ability to mediate the clearance of apoptotic cells and virus entry (3–9).

TIM proteins consist of four major domains: an N-terminal variable immunoglobulin-like (IgV) head domain, a stalk-like mucin domain that varies in length and O-glycosylation, a transmembrane domain, and a cytoplasmic domain. Of these, the IgV domain contains a high-affinity binding site for PS. TIM proteins are expressed on professional phagocytes such as macrophages and dendritic cells as well as lymphocytes. They are also expressed on nonprofessional phagocytes, including epithelial cells of various tissues, and mediate clearance of neighboring cells when they undergo apoptosis (8, 10). While TIM-family members directly bind PS (4), TAM-family receptors bind PS indirectly via soluble mediators, namely, growth arrest specific gene 6 (GAS6) or protein S (PROS) present in the serum and other bodily fluids (11–13). Inter- and intraspecies interactions between TAM-family receptors and these ligands are complex. Focusing on human and bovine ligands, whereas human GAS6 binds all three members of the human TAM family, human and bovine PROS exhibit weak binding to human TAM-family members with affinity never being reported for AXL (11–16). The C-terminal halves of GAS6 and PROS bind TAM receptors, and their N-terminal halves contain a γ-carboxylglutamic acid (Gla) domain that binds PS in a calcium-dependent manner. The Gla domain is enriched with glutamic acids that are posttranslationally modified by vitamin K-dependent γ-carboxylation, essential for the binding of calcium and PS (5, 17). Thus, for a virus to use a TAM receptor as an entry factor, it first needs to bind γ-carboxylated GAS6 or PROS.

Although not as well documented as PS, phosphatidylethanolamine (PE) is also sequestered to the inner leaflet of the plasma membrane (18, 19) and externalized when cells undergo apoptosis (19–21). We have previously shown that, like PS, PE was detected on the virions of enveloped viruses and could bind to a subset of the PS receptors (20). For example, TIM1 and annexin A5 bind PE as efficiently as or more efficiently than PS, and PE exposed on the apoptotic cells and virions enhances the clearance of apoptotic cells and virus entry, respectively. Similarly, CD300a, a cell-surface protein that is involved in immune responses and binds PE more efficiently than PS, also mediates infection of multiple viruses (7, 22). In addition, PE enhances the rate of blood clotting by lowering apparent PS concentrations required by blood-clotting factors (23–28). Despite extensive studies conducted in the past 4 decades on the role of PE in blood clotting, PE-PS synergy has not been investigated outside the blood coagulation field. Moreover, these previous studies solely utilized cell-free systems. Therefore, to extend these studies and our own previous observations, we investigated whether PE-PS cooperation contributes to PS receptor-mediated cellular processes such as virus entry and efferocytosis.

RESULTS

PS binding to GAS6, PROS, or TIM1 is enhanced by PE present on the same surface. We first extended PE-PS cooperation for PS binding to GAS6 and PROS, the PS-binding ligands of TAM-family receptors, in enzyme-linked immunosorbent assays (ELISAs). We also included in the assay a TIM-family member, TIM1, because of its distinct ability of binding PE as well as PS. Monomeric Ig-fusion forms of these proteins were used. For GAS6 and PROS, full-length proteins were fused to the Fc domain of human IgG1 (GAS6-Ig and PROS-Ig, respectively) containing mutations that prevented dimerization (see Fig. A1A in the appendix). In the case of TIM1, its ectodomain was fused to the Fc domain. When PC, PE, or PS was immobilized individually on ELISA plates, GAS6-Ig bound only to the PS-containing wells (Fig. 1A, left). However, when increasing amounts of PE were added to wells containing a fixed amount of PS, binding of GAS6-Ig was substantially increased, whereas PE alone in the absence of PS showed little or no binding in the wells containing the same amount of PE (Fig. 1B, left). Figure A1B in the appendix shows the ELISA in

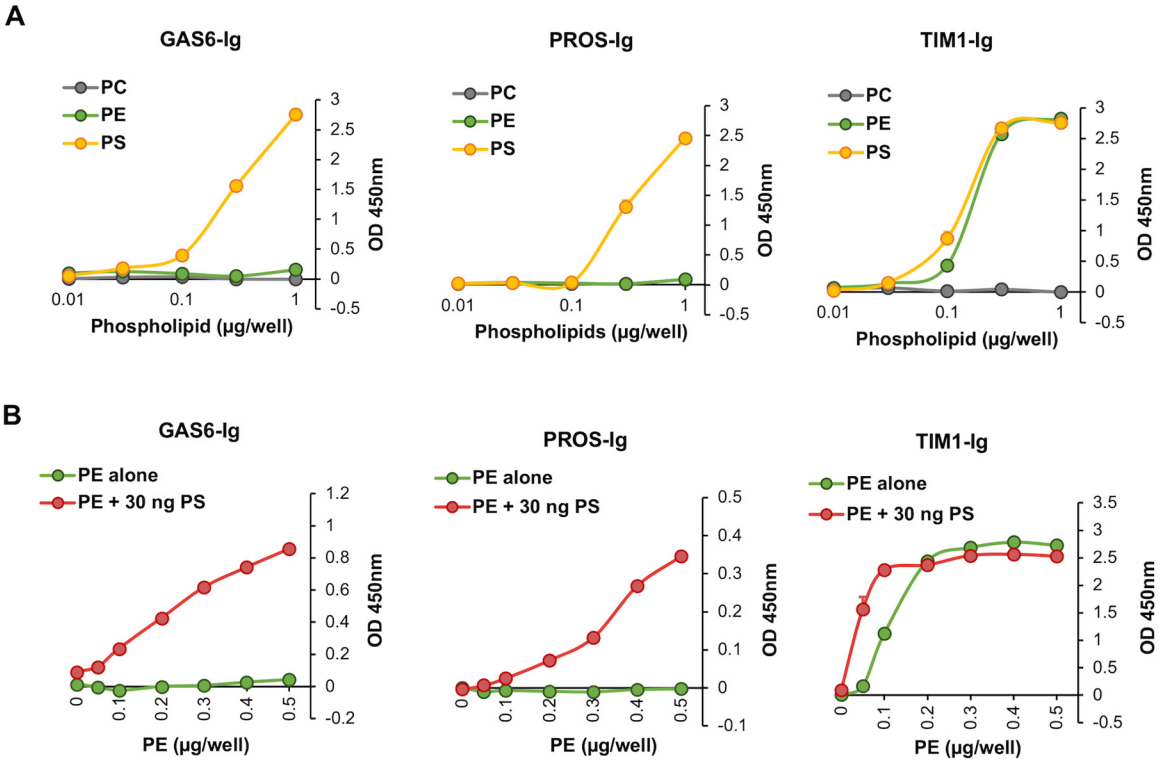

FIG 1 PS binding to GAS6, PROS, or TIM1 is enhanced by PE present on the same surface. (A) An increasing amount (0.01 to 1 μg per well) of the indicated phospholipid was dried on ELISA plates. Plates were incubated with 5 nM GAS6-Ig, PROS-Ig, or TIM1-Ig, and bound molecules were detected with an anti-human IgG antibody conjugated with HRP. Monomeric Ig-fusion proteins used in the assays are shown in Fig. A1A. (B) Similar to panel A except that a fixed amount (30 ng per well) of PS mixed with an increasing amount of PE (0 to 0.5 μg per well) or an increasing amount of PE alone was dried on the plates. Original binding assays presented in Fig. A1B include increasing amounts of both PE and PS. The data for increasing amounts of PS are excluded here to highlight PE-PS synergy. Representatives of three similar experiments are shown for panels A and B. Data are represented as means ± SDs.

which an increasing amount of PS was also included as a comparison. Similar results were obtained with PROS-Ig (Fig. 1A and B, middle). Interestingly, although TIM1-Ig naturally binds PE as well as PS (Fig. 1A, right), the combination of PE and PS in the same wells again enhanced total binding (Fig. 1B, right). Specifically, its binding of PE and PS when they were present together was substantially higher than the sum of PS and PE binding separately. As expected from TIM1's ability to naturally bind PE, the degree of enhancement is much lower than that for GAS6 and PROS. These data are consistent with the previous studies on blood-clotting factors (23–26) and demonstrate that PE-PS synergy extends beyond blood-clotting factors to TIM- and TAM-family PS-binding proteins.

PE synergizes with PS for GAS6-mediated liposome binding to AXL on the cell surface. Phospholipids immobilized on ELISA plates do not fully emulate the organization, curvature, and fluidity of biological membranes. In contrast, liposomes are large vesicles that are widely used as biomembrane substitutes. We therefore validated the ELISA observations using fluorescent liposomes and AXL-expressing cells. To assess PE-PS synergy in GAS6 binding, various liposomes were prepared (Fig. 2A). PS liposomes or PE liposomes were prepared with the indicated amounts of PS or PE, respectively, and with the remainder provided by phosphatidylcholine (PC). Note that PS and PE liposomes contain PC because, unlike PC, the PE and PS cannot form liposomes by themselves. Liposomes containing both PS and PE were made with fixed amounts of PS and increasing amounts of PE, again with PC filling in the remainder [referred to as "(PS+PE) liposomes" here] (Fig. 2A). Throughout the study, we compared these (PS+PE) liposomes to the mixtures of PE liposomes and PS liposomes [referred to "(PS)+(PE) liposomes" here]. For example,

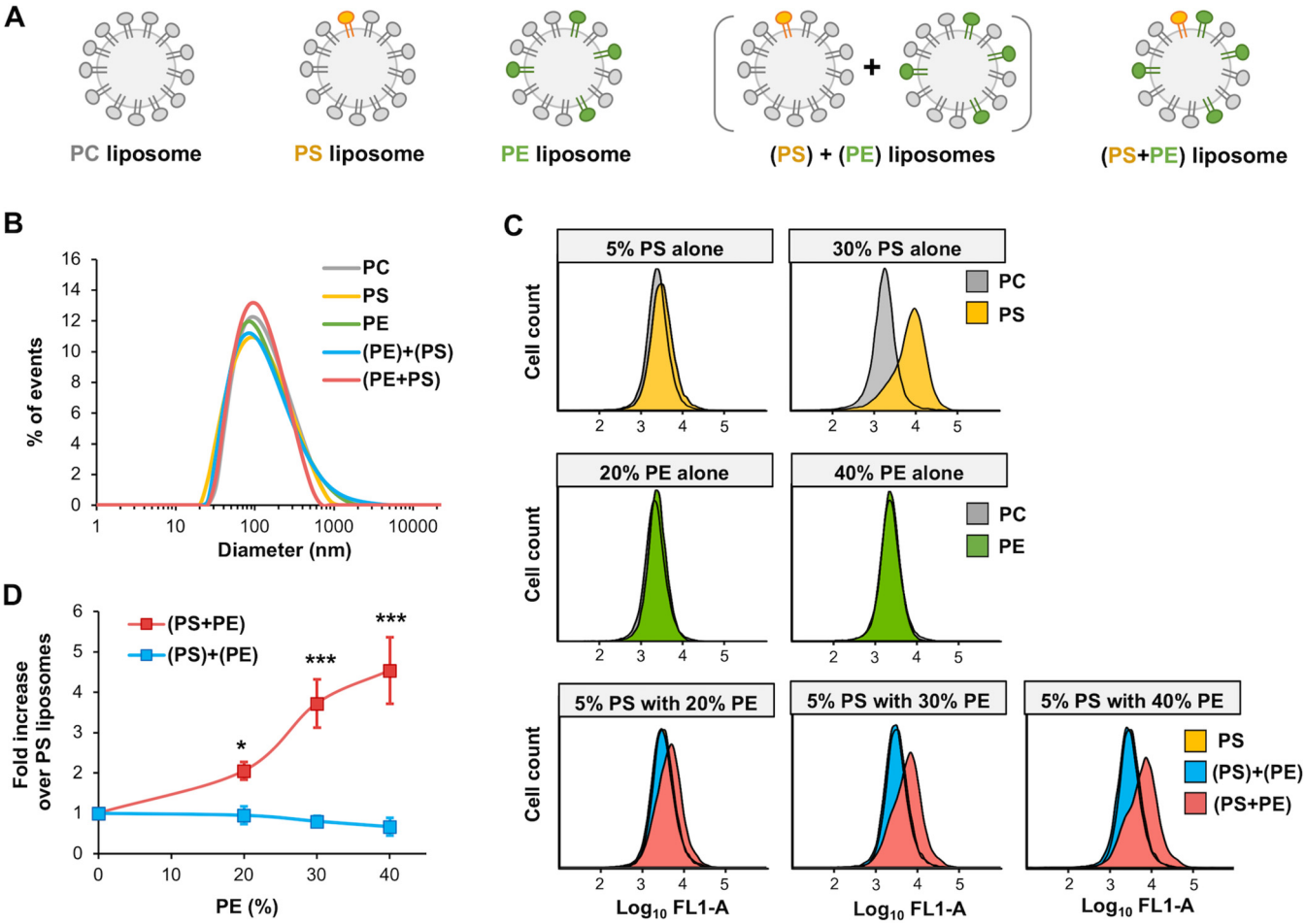

FIG 2 PE synergizes with PS for GAS6-mediated liposome binding to AXL expressed on the cell surface. (A) Diagrams showing the definitions and names of various liposomes used in the study. PC liposomes were made only with PC, and PS liposomes or PE liposomes were made of the indicated amount of PS or PE, respectively, with the remainder provided by PC. (PS)+(PE) liposomes are simply the mixtures of PS liposomes and PE liposomes of the indicated amount. (PS+PE) liposomes contain a fixed amount of PS and the indicated amount of PE with the rest provided by PC. (B) Liposomes were evaluated for size distribution by dynamic light scattering. Shown are representatives of two independent liposome preparations, each measured in three technical replicates. (C) AXL-293T cells were gently detached from culture flasks using citrate buffer, washed once with PBS, and incubated in V-bottom 96-well plates with 1 μM indicated liposomes in 100 μl of binding buffer supplemented with 10% FBS. After 15-min incubation on ice, cells were washed twice with binding buffer containing 10% FBS and twice without FBS and analyzed by flow cytometry. PC liposomes contain 99% PC and 1% TopFluor-PE, and 5% PS liposomes contain 5% PS, 94% PC, and 1% TopFluor-PE. Thirty percent PS liposomes contain 30% PS, 69% PC, and 1% TopFluor-PE. PE liposomes are made with the indicated amount of PE and 1% TopFluor-PE with PC to make up the rest. All (PS+PE) liposomes contain 5% PS, the indicated amount of PE, 1% TopFluor-PE, and PC to make up the rest. (PS)+(PE) liposomes are simply the mixtures of 1 μM PS liposomes and 1 μM PE liposomes of the indicated amount. Liposomes with 5% or 30% PS alone and 20% or 40% PE alone (the rest was made up with PC) were used as positive and negative controls. A representative of three independent experiments is shown. (D) (PS+PE) liposome and (PS)+(PE) liposome binding to AXL-293T cells normalized by the binding of PS liposomes to the same cells is shown as fold increase. The averages $\pm$ SD from three independent experiments including that shown in panel B are presented. The statistical significance of the difference between (PS+PE) and (PS)+(PE) conditions at various PE concentrations was determined by two-way ANOVA. *, $P < 0.05$; ***, $P < 0.001$.

to control for 1 μM (PS+PE) liposomes containing 5% PS and 20% PE, we used 2 μM 5% PS liposomes mixed with the same volume of 2 μM 20% PE liposomes, resulting in a mixture containing each of the PE and PS liposomes at 1 μM final concentration. The higher concentration of liposomes under the (PS)+(PE) condition (2 μM in total) was necessary to supply the same amount of PS and PE as under the (PS+PE) condition. All liposomes contain 1% of TopFluor-PE, a PE conjugated in its head group with a fluorophore, TopFluor. Because its head group is modified, TopFluor-PE does not function as PE but only provides fluorescence to the liposomes. When measured by dynamic light scattering, all liposomes displayed a wide range in size (30 to 600 nm), but these liposomes shared similar sizes with their peaks observed at 168 nm $\pm$ 26 nm (Fig. 2B).

To assess GAS6-mediated liposome binding to AXL, fetal bovine serum (FBS) was used as the source of GAS6, which is produced by endothelial cells and vascular smooth muscle cells (29, 30) and might be released into the circulation. Although the concentration of PROS (~350 nM) is much higher than that of GAS6 (~0.2 to 0.5 nM) in normal serum (31–33), as human and bovine PROS do not bind human AXL (11, 16), GAS6 is the sole ligand present in FBS for human AXL. HEK293T cells stably expressing AXL (AXL-293T) were incubated for 15 min on ice with liposomes in the binding buffer containing 10% fetal bovine serum (FBS). The binding buffer also contained 10 mM $CaCl_2$, required for the PS binding to GAS6. Cells were washed, and bound liposomes were measured by flow cytometry. As the top two panels of Fig. 2C show, 5% PS liposomes bound at a low but detectable level, while 30% PS liposome bound with high efficiency to AXL-293T cells. Neither 20% nor 40% PE liposomes detectably bound to the same cells. However, (PS+PE) liposomes, containing 5% PS and 20 to 40% PE, bound to the AXL-293T cells with substantially greater efficiency (Fig. 2C, bottom panels). In contrast, (PS)+(PE) liposomes containing the same amount of PS and PE bound similarly to 5% PS liposomes by themselves. The data from similar experiments were averaged and presented in Fig. 2D; binding of (PS+PE) liposomes to AXL-293T cells was 2- to 5-fold higher than that of (PS)+(PE) liposomes.

PE synergizes with PS for GAS6-mediated liposome uptake by AXL-expressing cells. The primary physiological function of PS receptors is to remove apoptotic cells by inducing efferocytosis. Accordingly, we next investigated whether PE-PS synergy can indeed contribute to this biological process. Because the amount of externalized PE and PS on the surface of the apoptotic cells cannot be easily measured or modulated, we used liposomes of known PE and PS content as surrogates for apoptotic cells in an efferocytosis-like assay in which GAS6/AXL-mediated liposome internalization was measured. AXL-293T cells on 48-well plates were incubated for 15 min on ice with 1 μM the indicated liposomes in the binding buffer supplemented with 10% FBS and transferred to a 37°C CO_2 incubator for 2 h to allow internalization of the bound liposomes. Cells were washed with a glycine buffer (pH 3.0) and thoroughly trypsinized to completely remove the liposomes that were bound to the cell surface but not yet internalized. Mock-293T cells that do not express AXL but were otherwise treated identically to AXL-293T cells, including drug selection, were included in the assay as a negative control. As the right panel of Fig. 3A shows, while the internalization of (PS)+(PE) liposomes by AXL-293T cells was as low as that of PS liposomes by themselves, (PS+PE) liposomes were internalized at much higher efficiency. None of the PS, (PS)+(PE), or (PS+PE) liposomes were internalized by Mock-293T cells above the background level exhibited by PC liposomes (Fig. 3A, left). To confirm that liposome engulfment by the AXL-293T cells was mediated by GAS6 present in FBS, we performed similar assays using GAS6-Ig. AXL-293T cells were incubated with the indicated liposomes together with GAS6-Ig in place of 10% FBS. "No GAS6," in which neither FBS nor GAS6-Ig was provided, was included as a negative control. As Fig. 3B shows, 5 nM GAS6-Ig mediated a comparable level of (PS+PE) liposome uptake as did 10% FBS, while no uptake was observed with any liposome in the absence of GAS6-Ig or FBS. Averages of similar experiments are presented in Fig. 3C. These data show that PE-PS synergy contributes to GAS6-mediated liposome internalization by AXL-293T cells.

PE synergizes with PS for inhibiting GAS6/AXL-mediated virus entry. AXL is well characterized for supporting the infection of many enveloped viruses (7, 20, 34–45). Accordingly, we next assessed the contribution of PE-PS synergy in GAS6/AXL-mediated virus entry. To do so, we verified that GAS6 could directly bind viruses and that this binding is dependent on its interaction with virion lipids but not with viral proteins. We first confirmed that GAS6 produced from HEK293T cells was functional with respect to its ability to bind PS. Specifically, we assessed the

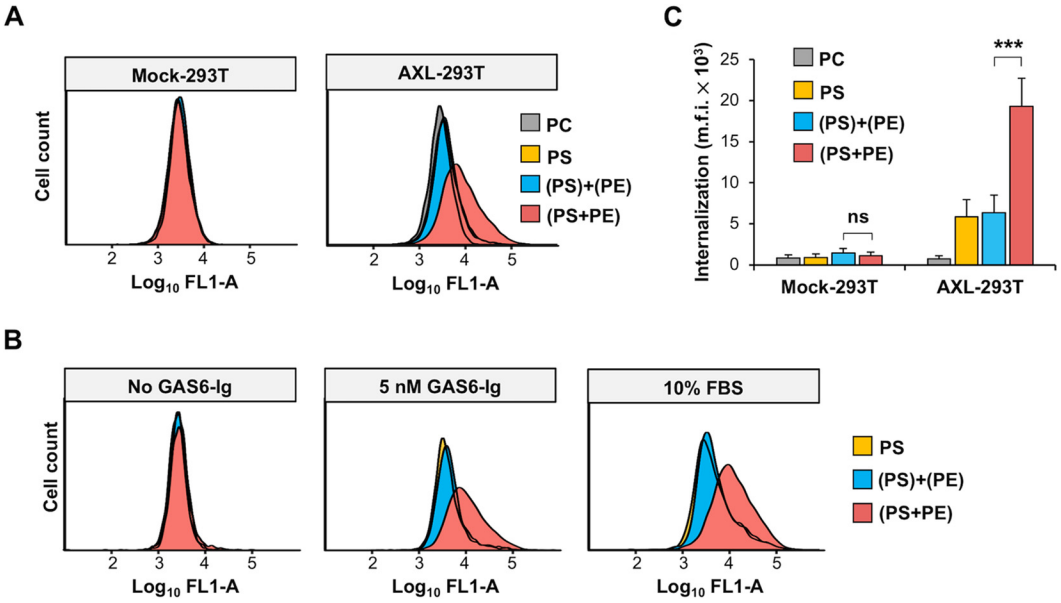

FIG 3 PE synergizes with PS for GAS6-mediated liposome uptake by AXL-expressing cells. (A) Mock-293T or AXL-293T cells grown on 48-well plates were incubated on ice for 15 min with 5 μM indicated liposomes in 200 μl of binding buffer supplemented with 10% FBS. Plates were transferred to a 37°C CO_2 incubator, and incubation was continued for 2 h. Cells were washed twice with acid and once with PBS and thoroughly trypsinized with 0.25% trypsin for 15 min at room temperature to completely remove liposomes that were attached to cells but not internalized. Detached cells were washed and analyzed by flow cytometry. Note that there is no binding in Mock-293T cells by any liposome above the background indicated by PC liposome binding. Also note that binding of PS liposomes and that of (PS)+(PE) liposomes in AXL-293T cells are overlapped. Shown are representatives of three independent experiments. (B) Similar to panel A except that liposome binding assays were performed with AXL-293T cells to compare GAS6-Ig and FBS. Binding buffer was supplemented either with 5 nM GAS6-Ig and 5% BSA or with 10% FBS. Shown are representatives of five independent experiments. (C) The averages ± SD from five liposome-internalization experiments including the one shown in panel B are presented. The statistical significance of the difference between the (PS)+(PE) and the (PS+PE) conditions was separately determined in Mock-293T and AXL-293T cells by one-way ANOVA. ***, $P < 0.001$; ns, $P > 0.05$; m.f.i., mean fluorescence intensity.

need for extra γ-glutamyl carboxylase (GGCX) and vitamin K supplementation, because γ-carboxylation of GAS6 Gla domain is carried out by GGCX and dependent on vitamin K (17, 37). HEK293T cells were transfected with a plasmid expressing GAS6-Ig with or without a plasmid encoding γ-glutamyl carboxylase (GGCX), and culture medium was supplemented or not with vitamin K. As the left panel of Fig. 4A shows, GAS6-Ig produced in the absence of vitamin K did not bind PS at any concentration in ELISAs, confirming that vitamin K is essential for γ-carboxylation. On the other hand, exogenous expression of GGCX did not boost PS binding by GAS6-Ig, suggesting that the endogenous level of GGCX enzyme is sufficient to produce functional GAS6 at least in HEK293T cells (Fig. 4A, right). We next verified that GAS6 binding to viruses was mediated via the interaction with virion PS, but not with viral proteins. We did so based on established knowledge and our own observation that GAS6 binding to PS, but not to proteins, is completely dependent on the presence of vitamin K during its production and calcium during binding assays. We thus produced GAS6-Ig from HEK293T cells under various conditions. Zika virus (ZIKV) was incubated with GAS6-Ig, virus particles bound to GAS6-Ig were precipitated using protein A-Sepharose beads, and captured viruses were analyzed by SDS-PAGE and visualized by Western blotting using an E protein-specific antibody. C-GAS6-Ig that lacks the Gla domain-containing N-terminal half of GAS6 was used as a negative control. Figure 4B shows that GAS6-Ig produced in the presence, but not in the absence, of vitamin K efficiently captured ZIKV. It also shows that virus binding to GAS6-Ig is critically dependent on calcium. C-GAS6-Ig did not capture any virus particle, and extra GGCX did not contribute to GAS6 binding to viruses.

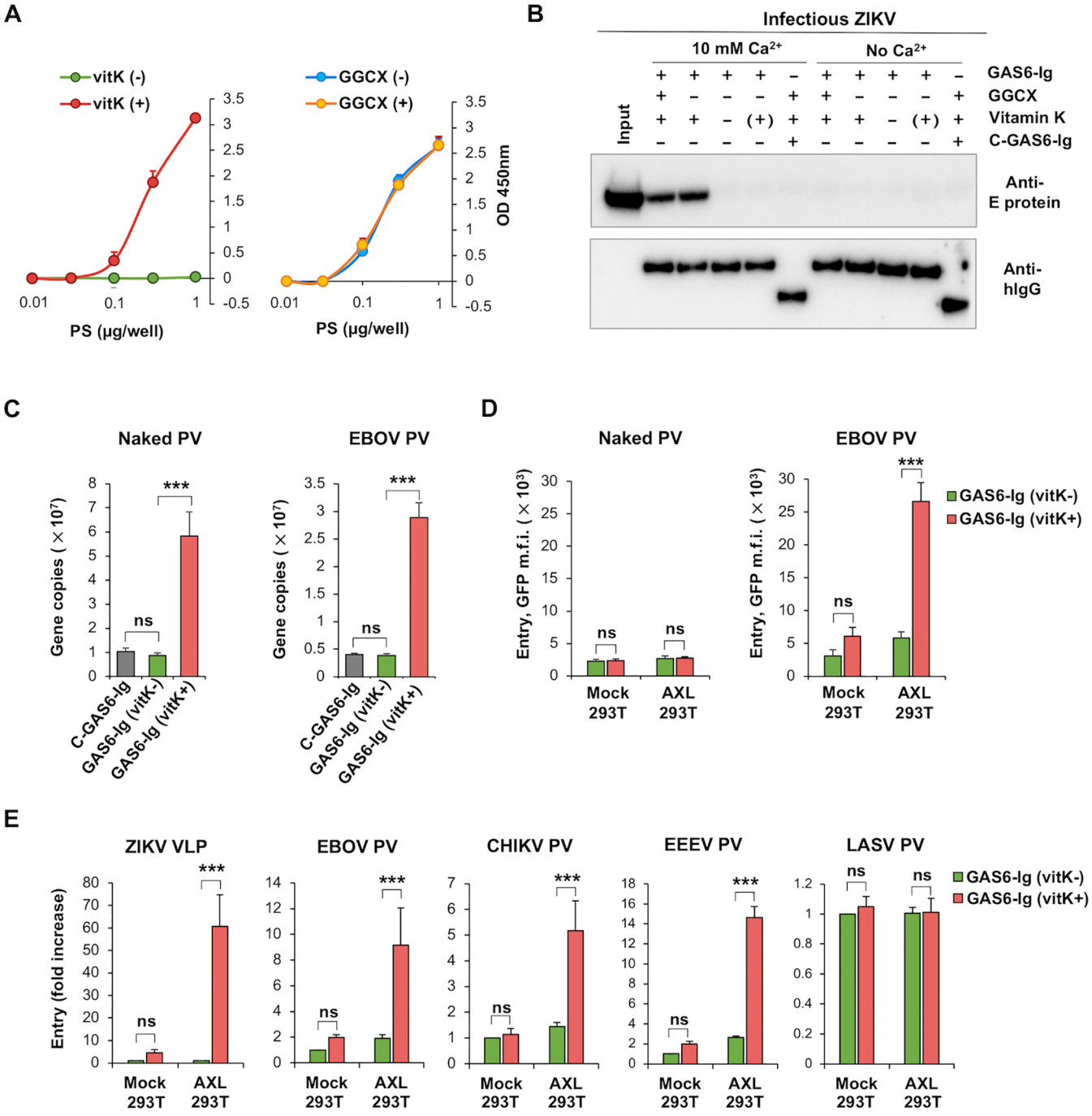

FIG 4 AXL-mediated virus infection is dependent on γ-carboxylation of GAS6. (A) Left panel: GAS6-Ig proteins produced from transfected HEK293T cells in the presence (vitK+) or absence (vitK−) of supplemented vitamin K were evaluated at 5 nM for their ability to bind PS in ELISAs as described in the legend to Fig. 1A. A representative of three similar results is shown. Right panel: GAS6-Ig proteins produced from transfected HEK293T cells with or without GGCX cotransfection were evaluated for their ability to bind PS as described in the legend to Fig. 1A. A representative of three similar results is shown. Note that in HEK293T cells, extra GGCX transfection is not necessary to produce functional GAS6, likely due to the sufficient level of endogenous GGCX in these cells. (B) GAS6-Ig proteins produced from HEK293T cells in the presence and absence of GGCX and vitamin K supplementation were used to capture ZIKV in the presence or absence of 10 mM $CaCl_2$. Captured viruses were precipitated by protein A-Sepharose beads and analyzed by nonreducing and reducing SDS-PAGE. The nonreducing gel was transferred to PVDF membranes and blotted with 4G2 antibody that recognizes flavivirus E protein (top). The reducing gel was blotted with an anti-human IgG antibody (bottom). The E protein band shown in the first lane indicates the amount of input virus used in the assay. "(+)" indicates that vitamin K was added during the capture assay but not during GAS6-Ig production. (C) A similar experiment as that shown in panel B except that naked and EBOV PVs are used, and bound PVs were quantified by RT-qPCR. (D) The same naked and EBOV PVs were assessed in entry experiments in Mock- or AXL-293T cells in the presence of GAS6 produced in the presence or absence of vitamin K. (E) Mock- or AXL-293T cells were incubated in a 37°C CO_2 incubator for 1 h with the ZIKV VLP or EBOV, CHIKV, EEEV, or LASV PV in the presence of 3 nM GAS6-Ig proteins produced with or without supplemented vitamin K and analyzed 24 h later for eGFP expression. The statistical significance of the difference between the presence and absence of vitamin K during GAS6-Ig production was determined by one-way ANOVA for panel C or two-way ANOVA for panels D and E. ***, $P < 0.001$; **, $P < 0.01$; ns, $P > 0.05$.

Although vitamin K-dependent binding indicates that GAS6 binding to ZIKV is mediated by PS, not by a protein (17, 37), we verified it using naked PV that was produced in the same way as other pseudoviruses (PVs) but without the viral entry protein. Naked PV and Ebola virus (EBOV) PV were preincubated with GAS6-Ig and precipitated with protein A-Sepharose beads, and bound virions were quantified by reverse transcription-quantitative PCR (RT-qPCR). GAS6-Ig produced in the absence of vitamin K and C-GAS6-Ig were used as negative controls. As shown in Fig. 4C, naked PV bound GAS6-Ig, but not C-GAS6-Ig or GAS6-Ig produced in the absence of vitamin K, more efficiently than the same amount of EBOV PV. Of note, although naked PV binds GAS6-Ig with high efficiency, it is not able to enter cells using AXL/GAS6, due to the lack of any viral entry protein, while EBOV PV efficiently enters cells (Fig. 4D). Together, these data indicate that GAS6 binding to viruses is mediated by its interaction with virion PS but not with viral proteins.

We then verified that GAS6-Ig promoted AXL-mediated virus infection. To exclude the impact of downstream steps in viral replication, we used virus-like particles (VLP) or pseudoviruses (PVs). ZIKV VLP was produced from 293T cells by transfecting a plasmid expressing green fluorescent protein (GFP) and nonstructural proteins of West Nile virus (WNV) and a plasmid encoding WNV capsid and ZIKV prM and E proteins. PVs were produced by pseudotyping murine leukemia virus structural proteins with the entry protein of Ebola virus (EBOV), Chikungunya virus (CHIKV), eastern equine encephalitis virus (EEEV), or Lassa fever virus (LASV). Mock- or AXL-293T cells were then infected with these VLP or PVs in the presence of GAS6-Ig produced with or without vitamin K supplementation. GAS6-Ig produced in the presence of vitamin K, but not that produced without vitamin K, enhanced AXL-mediated entry of ZIKV VLP and EBOV, EEEV, and CHIKV PVs (Fig. 4E), indicating that virion PS, not viral protein, was involved in the GAS6/AXL-mediated virus entry (5). As expected, LASV PV entry was not affected by GAS6 or AXL, because LASV does not use PS receptors, at least in HEK293T cells (20, 34), although LASV was shown to use PS receptors in other cell lines (46).

Having shown that GAS6-Ig mediates virus infection of AXL-expressing cells and that GAS6 binding to virus is mediated by its interaction with virion PS, we next assessed the contribution of PE-PS synergy to GAS6/AXL-mediated virus entry. As with apoptotic cells, it is difficult to manipulate PE and PS content of viruses, and we therefore assessed PE-PS synergy by measuring liposome-mediated inhibition of viral infection into AXL-293T cells. We first assessed PE-PS synergy in ZIKV infection. Infectious ZIKV was preincubated in serum-free Dulbecco's modified Eagle's medium (DMEM) with the indicated liposomes and GAS6-Ig. Mock- and AXL-293T cells were infected with the preincubation mix for 1 h, and infection level was analyzed 18 h later. As Fig. 5A shows, while both PS liposomes and (PS)+(PE) mixed liposomes modestly inhibited ZIKV infection of AXL-293T cells, inhibition by (PS+PE) liposomes was substantially increased. We then extended this observation to other viruses by using PVs. ZIKV VLP was used as a positive control, and LASV PV was as a negative control. VLP and PVs were preincubated with liposomes and GAS6-Ig and incubated with Mock- or AXL-293T cells for 1 h. Cells were analyzed 24 h later for enhanced GFP (eGFP) expression. While PS liposomes and (PS)+(PE) mixed liposomes similarly inhibited approximately 40% of ZIKV VLP entry into AXL-293T cells, inhibition by (PS+PE) liposomes was greatly increased to 98% (Fig. 5B). Similar patterns of inhibition were observed with EBOV, CHIKV, and EEEV PVs, albeit the degree of synergy was somewhat lower than that observed for ZIKV VLP. As expected, infection by LASV PV was not inhibited by any liposome. These data clearly demonstrate that the presence of PE in the same liposomes as PS enhances the ability of liposomes to inhibit GAS6/AXL-mediated virus entry.

DISCUSSION

We report here that PE when present together with PS enhances PS binding to PS receptors and that this PE-PS synergy contributes to the efficiency of biological

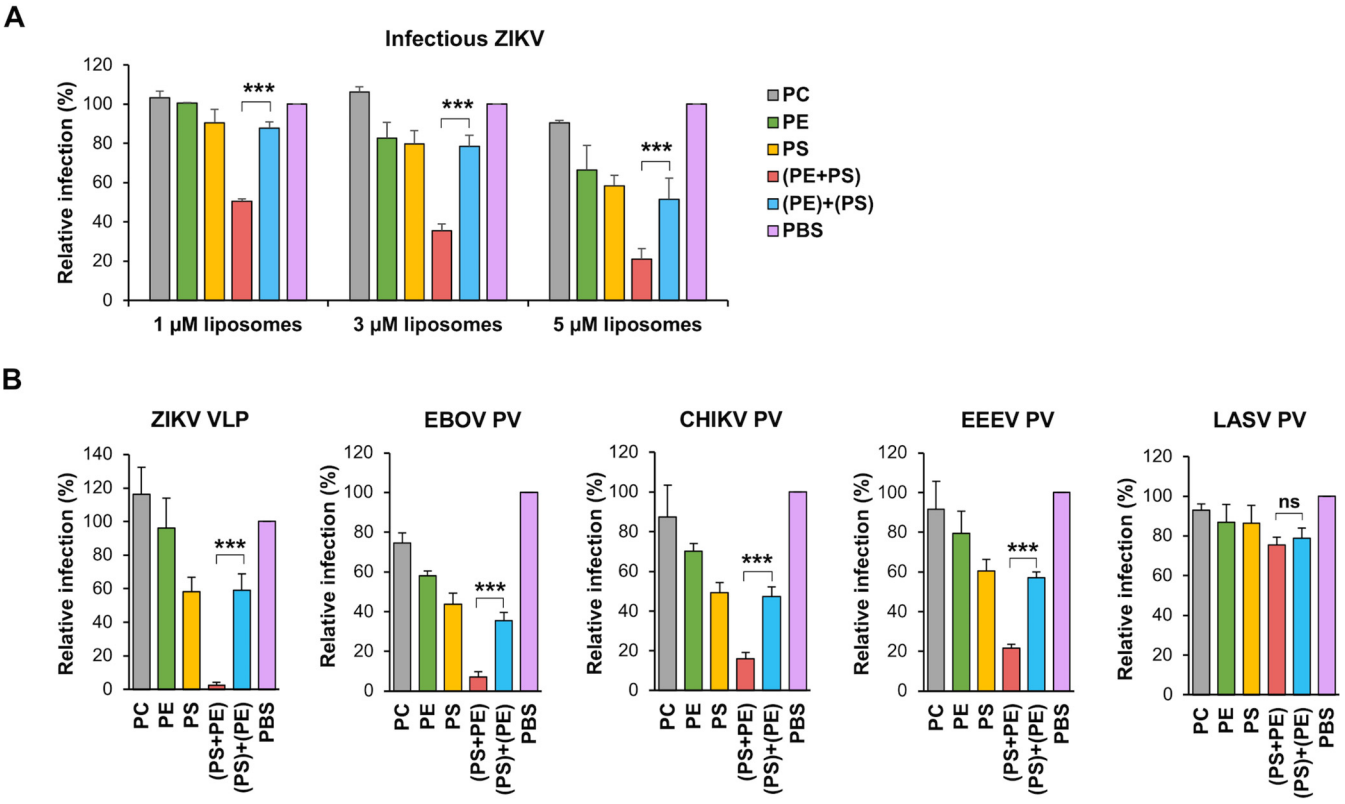

FIG 5 PE synergizes with PS for inhibiting GAS6/AXL-mediated virus entry. (A) AXL-293T cells were infected with replication-competent ZIKV preincubated with 3 nM GAS6-Ig and 1, 3, or 5 μM indicated liposomes. Inoculum was replaced 1 h later with fresh medium, and infection level was analyzed 18 h later by staining permeabilized cells with the pan-flavivirus antibody, 4G2. (B) The entry of ZIKV VLP or EBOV, CHIKV, EEEV, or LASV PV into AXL-293T cells was performed. VLP or PVs were preincubated with 5 μM liposomes and 3 nM GAS6-Ig. The preincubation mix was added to cells at 37°C in a CO_2 incubator and replaced 1 h later with complete medium, and infected cells were analyzed 24 h postinfection. (A and B) Averages ± SD from three independent experiments are shown. The statistical significance of the differences between the (PS)+(PE) and (PS+PE) conditions was determined by one-way ANOVA. ***, $P < 0.001$; ns, $P > 0.05$.

processes such as efferocytosis and virus entry mediated by PS receptors. For example, the presence of PE and PS on the same liposomes increased liposome binding to GAS6 and internalization mediated by GAS6/AXL. This PE-mediated enhancement is not due to direct binding of PE to GAS6, because GAS6 does not bind PE at any concentration. Interestingly, we also observed PE-PS synergy with hTIM1, a receptor that binds PE as efficiently as it binds PS. In this case, however, synergy between PS and PE was less pronounced and was observed only in a cell-free assay. In fact, we could not detect PE-PS synergy in cell-based assays for hTIM1-mediated efferocytosis or virus entry. It is likely that low-level synergy was masked by the higher additive effects, whereby TIM1 directly binds both phospholipids.

Many PS receptors participate in efferocytosis. Although different families of PS receptors are expressed in different tissues, members of the same family are often expressed in the same tissues, organs, or cells. It is unclear why such redundancy is necessary to clear apoptotic cells. It is tempting to speculate that these receptors are differentially regulated and that distinct recognition patterns of PE and PS help to convey different signals that lead to engulfing cells and immune silencing. It remains unclear exactly how PE amplifies PS binding to GAS6, but there are a few possible mechanisms. It is possible that the presence of PE in the same membrane as PS could induce the formation of PS-rich microdomains that is more favorable for GAS6 binding (Fig. 6A), as has previously been suggested for blood-clotting factors (25). It is also possible that interaction of PE with neighboring PS alters the conformation of PS, making it more suitable for GAS6 binding (Fig. 6B). Alternatively, although native GAS6 does not bind PE, PS binding to GAS6 may induce a

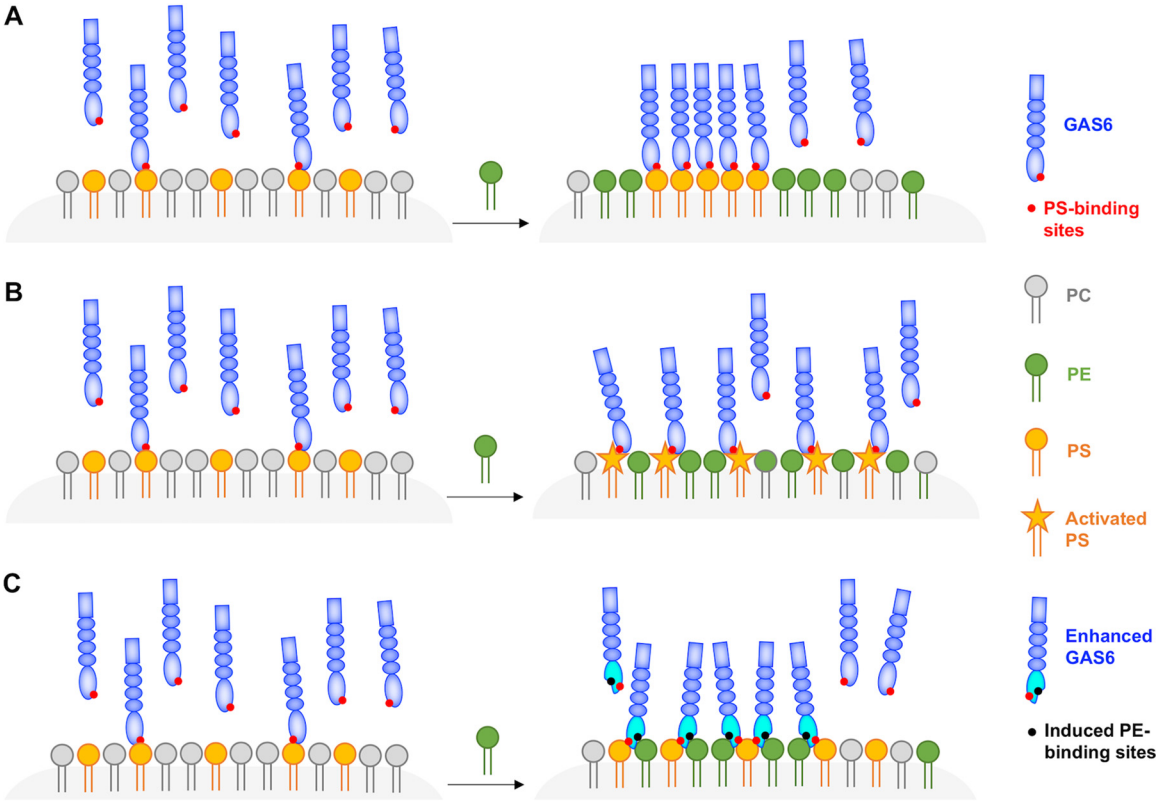

FIG 6 Possible mechanisms for PE and PS synergy for GAS6 binding. (A) Presence of PE on the same surface or membrane as PS may induce PS-enriched microdomains, and PS molecules in the microdomains are more favorable for GAS6 binding. (B) Interaction of PE with neighboring PS may alter the conformation of PS, rendering it more suitable for GAS6 binding. (C) Unliganded GAS6 does not bind PE, but PS binding to its Gla domain may induce cryptic PE-binding sites unmasked on GAS6.

novel PE-binding site unlocked on GAS6 (Fig. 6C). Regardless, it is clear that PE can substantially amplify PS binding to GAS6, and perhaps also to TIM1 through a somewhat different mechanism.

The membrane of enveloped viruses derives from the cellular membrane from which they bud. The PE content of mammalian membranes is much higher than that of PS, and PE content is higher in the endoplasmic reticulum (ER) than in the plasma membrane. Specifically, PS constitutes 8 to 10% of the plasma membrane and 3 to 5% of the ER membrane, whereas PE constitutes 20 to 25% and 25 to 30%, respectively, of the plasma and ER membranes. Because PE-induced enhancement of PS binding to PS receptors is proportional to PE content, viruses that bud from the ER membrane, such as flaviviruses, may depend more on PE-PS synergy, especially with their lower PS contents, than those that bud from the plasma membrane. PE content is even higher in insect cells than in the ER membrane of mammalian cells, comprising up to 60% of total phospholipids (47). Thus, the role of PE may be even more important when arboviruses such as alphaviruses and flaviviruses are transmitted from their insect vectors to humans.

MATERIALS AND METHODS

Cell lines and plasmids. Human embryonic kidney HEK293T and Vero cells were obtained from the ATCC and maintained in high-glucose DMEM supplemented with 10% FBS at 37°C with 5% CO_2. HEK293T cells transduced to stably express AXL (AXL-293T) or mock transduced (Mock-293T) were selected and maintained in medium supplemented with 0.5 μg/ml puromycin (InvivoGen). All cells were free of mycoplasma and maintained in medium containing 5 μg/ml Plasmocin (InvivoGen).

The plasmid expressing AXL was generated by cloning the cDNA fragment encoding human AXL (GenBank accession no. AAH32229.1) into the retroviral vector pQCXIP (Clontech). The vector for AXL transduction was produced by transfecting pQCXIP-AXL into HEK293T cells together with the plasmid

encoding murine leukemia virus gag-pol and that encoding the G protein of vesicular stomatitis virus. The vector for mock transduction was produced similarly using empty pQCXIP plasmid.

The expression plasmids for GAS6-Ig and PROS-Ig were generated by cloning the cDNA fragments encoding full-length human GAS6 (GenBank accession no. AAH38984.1) or PROS (GenBank accession no. AAH15801.1) into the pcDNA3.1(+) containing CD5 signal peptide and the genomic sequence of the human IgG1 Fc region that contains six mutations (C310A, C316N, C319G, L368R, F495H, and Y407E) to prevent dimerization. The plasmid expressing the Ig-fusion form of the C-terminal half of GAS6 was generated by cloning cDNA encoding its residues 279 through 678 into the same monomeric Ig-fusion vector. The expressor plasmid of GGCX was generated by cloning its cDNA sequence into pQCXIP. For the plasmid expressing TIM1-Ig, the ectodomain of human TIM1 (residues 1 to 290, GenBank accession no. AAC39862.1) was cloned into the same Ig-fusion plasmid.

Phospholipid ELISA. The following synthetic phospholipids (Avanti Polar Lipids) were used in assays: 12-dioleoyl-sn-glycero-3-phosphocholine (PC), 12-dioleoyl-sn-glycero-3-phosphoethanolamine (PE), and 12-dioleoyl-sn-glycero-3-[phospho-L-serine] (PS). To assess phospholipid-binding profiles of the Ig-fusion proteins, phospholipids in chloroform in the original vials were dried out and resuspended and diluted in methanol. The indicated amounts of phospholipids in 100 μl were added to each well of the plates and air dried overnight—it is important to dry out completely—in polystyrene ELISA plates. The plates were washed with Tris-buffered saline (TBS: 25 mM Tris base, 137 mM NaCl, 2.7 mM KCl, pH 7.4) containing 10 mM $CaCl_2$ and 0.05% (vol/vol) Tween 20 (TBST), blocked for 1 h at room temperature with 1% bovine serum albumin (BSA) in TBS, and washed with TBST. The plates were then incubated for 1 h at room temperature with the indicated amounts of Ig-fusion proteins diluted in TBS containing 10 mM $CaCl_2$ (TBS-Ca^{2+}) and washed with TBST containing 10 mM $CaCl_2$ (TBST-Ca^{2+}) before incubated with a horseradish peroxidase (HRP)-conjugated goat anti-human IgG (Jackson Immuno Research Laboratories). The plates were extensively washed with TBST-Ca^{2+} and TBS-Ca^{2+} before binding was visualized using UltraTMB substrate (Thermo Scientific Pierce). The reaction was terminated with 2 M phosphoric acid, and the plates were read at 450 nm with a SpectraMax Paradigm microplate reader (Molecular Devices). Wells treated the same way but only coated with methanol were used as background controls.

Ig-fusion protein production. To produce monomeric Ig-fusion proteins, the appropriate plasmid was transfected into HEK293T cells using the calcium-phosphate method and cultured in FreeStyle 293 medium (Thermo Fisher). To produce monomeric GAS6-Ig, its expression plasmid was transfected into HEK293T cells with or without the plasmid encoding GGCX at a ratio of 3:1, and cells were cultured in FreeStyle 293 medium supplemented with 10 μg/ml vitamin K_1 (Sigma). The culture supernatants were harvested 72 h posttransfection, clarified by 0.45-μm filtration, and quantified by Coomassie blue staining following SDS-PAGE, using purified human Ig as a standard. Mock-transfected culture supernatant was similarly produced by transfecting cells with an empty plasmid and used in place of GAS6-Ig as a negative control.

Liposome preparation and size measurement. To prepare liposomes, phospholipids in chloroform were dried and resuspended in methanol. They were combined as needed in glass vials together with 1 mol% of a fluorescent phospholipid (12-dioleoyl-sn-glycero-3-phosphoethanolamine labeled in the head group with TopFluor) (Avanti Polar Lipids) and dried again. The lipid films were hydrated by adding phosphate-buffered saline (PBS) and vigorously vortexing for 1 h at room temperature. The vesicle suspensions were left to stand overnight, and next day, the formed large multilamellar vesicles were downsized by bath sonication until the suspensions were clarified. The time required to clarify 1 ml liposomes typically ranges from 15 to 20 min for PE and PS and 1 h for PC. Liposomes were stored at 4°C and used within a few weeks after sonication was reapplied for each use.

Size distribution of liposomes was measured with the DynaPro NanoStar dynamic light scattering detector (Wyatt Technology). Briefly, liposome suspensions at a concentration of 0.4 mg/ml in PBS were centrifuged for 5 min at 1,000 $\times$ *g* to pellet any particulate impurities. Next, 7.5 μl of the supernatant was loaded into a quartz cuvette and allowed to equilibrate to 25°C for 10 min in the sample chamber. After thermal equilibrium was reached and laser power and detector attenuation automatically adjusted, size measurement for each liposome was calculated from 10 acquisitions with 5-s integration time. Data were analyzed in Dynamics software version 7.10 (Wyatt Technology).

Liposome binding and internalization assay. For binding assays, Mock- and AXL-293T cells were detached with citrate buffer (15 mM sodium citrate, 135 mM KCl), washed once with PBS, and incubated in 96-well plates for 15 min on ice with the indicated liposomes in 100 μl of binding buffer (10 mM HEPES, 140 mM NaCl, 10 mM $CaCl_2$, pH 7.4) supplemented either with 10% FBS or with the indicated concentration of GAS6-Ig. If GAS6-Ig was used, binding buffer was supplemented with 5% bovine serum albumin (BSA) to block nonspecific binding. Cells were washed twice with binding buffer containing 10% FBS and twice without FBS, and analyzed by an Accuri C6 flow cytometer (BD Biosciences) equipped with HyperCyt autosampler (IntelliCyt).

For internalization assays, Mock- and AXL-293T cells attached on 48-well plates were incubated on ice for 15 min with the indicated liposomes in binding buffer supplemented with either 10% FBS or the indicated concentration of GAS6-Ig and 5% BSA. Plates were transferred to a 37°C CO_2 incubator, and incubation continued for 2 h. Cells were washed twice with acid (200 mM glycine, 150 mM NaCl, pH 3.0) and once with PBS and trypsinized with 0.25% trypsin to completely remove the liposomes that were not internalized. Cells were further washed twice with binding buffer containing 10% FBS and twice without FBS and analyzed by flow cytometry.

Liposome-mediated inhibition of infection by PV, VLP, and an infectious virus. ZIKV VLP was produced by transfecting HEK293T cells at a 1:2 ratio with the plasmid encoding the capsid of West

Nile virus (lineage II, strain B956) and prM and E proteins of ZIKV (Brazil, strain SPH2015) and the plasmid encoding eGFP and the nonstructural proteins 1 to 5 of West Nile virus (lineage II, strain B956) (20). Culture supernatants containing ZIKV VLP were harvested at 48 h posttransfection and clarified by 0.45-μm filtration. PVs were produced from HEK293T cells as previously described (34) by pseudotyping murine leukemia virus structural proteins with E1 and E2 proteins derived from EEEV (strain FL91-4697) or CHIKV (strain 37997), mucin domain-deleted glycoprotein (GP) derived from Zaire EBOV (strain Mayinga), or glycoprotein complex (GPC) derived from LASV (strain Josiah). PVs were harvested 33 to 34 h posttransfection. VLP and PVs were preincubated for 1 h in a 37°C CO_2 incubator with or without the indicated concentration of liposomes and GAS6-Ig in serum-free DMEM. Two hundred microliters of the preincubation mix was then added to the cells on 48-well plates and further incubated for 1 h, and the culture supernatants were replaced with fresh DMEM containing 10% FBS. Cells were analyzed for eGFP expression 24 h later by flow cytometry.

Infectious ZIKV (strain PB81, Brazil) was obtained from the World Reference Center for Emerging Viruses and Arboviruses (WRCEVA) and propagated in Vero cells. Culture supernatants of the infected cells were harvested at days 2 and 3 postinfection, cleared by 0.45-μm filtration, and frozen at −80°C. Virus preparations were quantified by RT-qPCR targeting the nonstructural protein NS3 [sense, 5′-TTAT GGACACCGAAGTGGAAG-3′; antisense, 5′-CACGCTTGGAACAAACCAAA-3′; probe, 5′-6-carboxyfluorescein (FAM)-TCAGGCTTTGA-(ZEN)-TTGGGTGACGGAT-Iowa black fluorescent quencher (IBFQ)-3′]. ZIKV was preincubated with the indicated concentrations of liposomes and GAS6-Ig in serum-free DMEM, and the preincubation mix containing 1×10^8 copies of ZIKV was used to infect AXL-293T cells in a 37°C CO_2 incubator. Inoculum was replaced 1 h later with fresh medium. Eighteen hours later, cells were fixed with 2% formaldehyde and permeabilized with 0.1% saponin, and infection level was assessed by flow cytometry (Accuri C6; BD Biosciences) of the cells stained with the pan-flavivirus antibody, 4G2, and anti-mIgG antibody conjugated with Alexa 647.

GAS6-mediated virus or PV capture assay. Infectious ZIKV (Brazil, strain PB81) obtained from World Reference Center for Emerging Viruses and Arboviruses was propagated in Vero cells and quantified by RT-qPCR. GAS6-Ig and C-Gas6-Ig were produced from HEK293T cells with or without GGCX cotransfection and vitamin K supplementation. Infectious ZIKV at 2×10^8 genome copies was incubated for 1 h at 37°C with 0.2 μg of GAS6-Ig or C-Gas6-Ig in 500 μl TBS in total supplemented or not with 10 mM $CaCl_2$. Protein A-Sepharose beads were added, and incubation was continued at room temperature for another hour with continuous rocking. Beads were washed 3 times with TBST and analyzed by nonreducing and reducing SDS-PAGE. Proteins on both gels were separately transferred to polyvinylidene difluoride (PVDF) membranes and blotted either with 4G2 antibody that recognizes flavivirus E protein (nonreducing gel) or with an anti-human IgG antibody (reducing gel) to visualize captured ZIKV and Ig-fusion proteins, respectively.

Naked PV and EBOV PV were produced from HEK293T cells by transfecting a retroviral vector expressing eGFP and plasmids encoding murine leukemia virus gag and pol, and viral entry protein at a ratio of 3:6:1. In the case of naked PV, the plasmid expressing a viral entry protein was replaced with an empty plasmid. Naked or EBOV PV at 1×10^9 genome copies was preincubated at room temperature for 1 h with 0.3 μg of GAS6-Ig or C-Gas6-Ig in 500 μl TBS in total supplemented or not with 10 mM $CaCl_2$. Protein A-Sepharose beads were added, and incubation was continued at room temperature for another hour with continuous rocking. After beads were washed 3 times with TBS, RNA was extracted using TRIzol and GlycoBlue coprecipitant and reverse transcribed using a high-capacity cDNA reverse transcription kit (Applied Biosystems). qPCR was performed using Luna Universal Probe qPCR Master Mix (New England Biolabs) with the known quantity of pQCXIX-eGFP vector to generate standard curves, and data were collected with CFX Manager 3.1 (Bio-Rad). qPCR primers and a probe targeting the eGFP gene were synthesized at Integrated DNA Technologies. Primers were as follows: sense primer, 5′-GAACCGCATCG AGCTGAA-3′; antisense primer, 5′-TGCTTGTCGGCCATGATATAG-3′; probe, 5′-FAM-ATCGACTTC-(ZEN)-AA GGAGGACGGCAAC-IBFQ-3′.

Statistics. The difference between groups was tested using either one-way or two-way analysis of variance (ANOVA) as indicated for each experiment. The null hypothesis was rejected when P was <0.05.

APPENDIX

Figure A1A shows the monomeric Ig-fusion proteins that were used in ELISAs shown in Fig. 1 and Fig. A1B. To prevent dimerization by Ig-fusion proteins, C310A, C316N, C319G, L368R, F495H, and Y407E mutations were introduced to the Fc domain. Dimeric GAS6-Ig is used as a control for reducing and nonreducing SDS-PAGE. Figure A1B shows PE-PS synergy for the binding by GAS6, PROS, and TIM1. GAS6 and PROS bind only PS, while TIM1 binds both PE and PS. When an increasing amount of PE was added to a small amount (30 ng/well) of PS, which by itself did not show detectable binding, these proteins exhibited substantially increased binding. An increasing amount of PS is included as a comparison. GAS6-Ig binding to 30 ng PS + PE reached nearly half of its binding to an increasing amount of PS, although it does not bind PE at all by itself. PE-PS synergy is also observed for PROS-Ig, albeit at a much lower level. Although TIM1 naturally binds both PE and PS, PE-PS synergy is still observed to a certain extent.

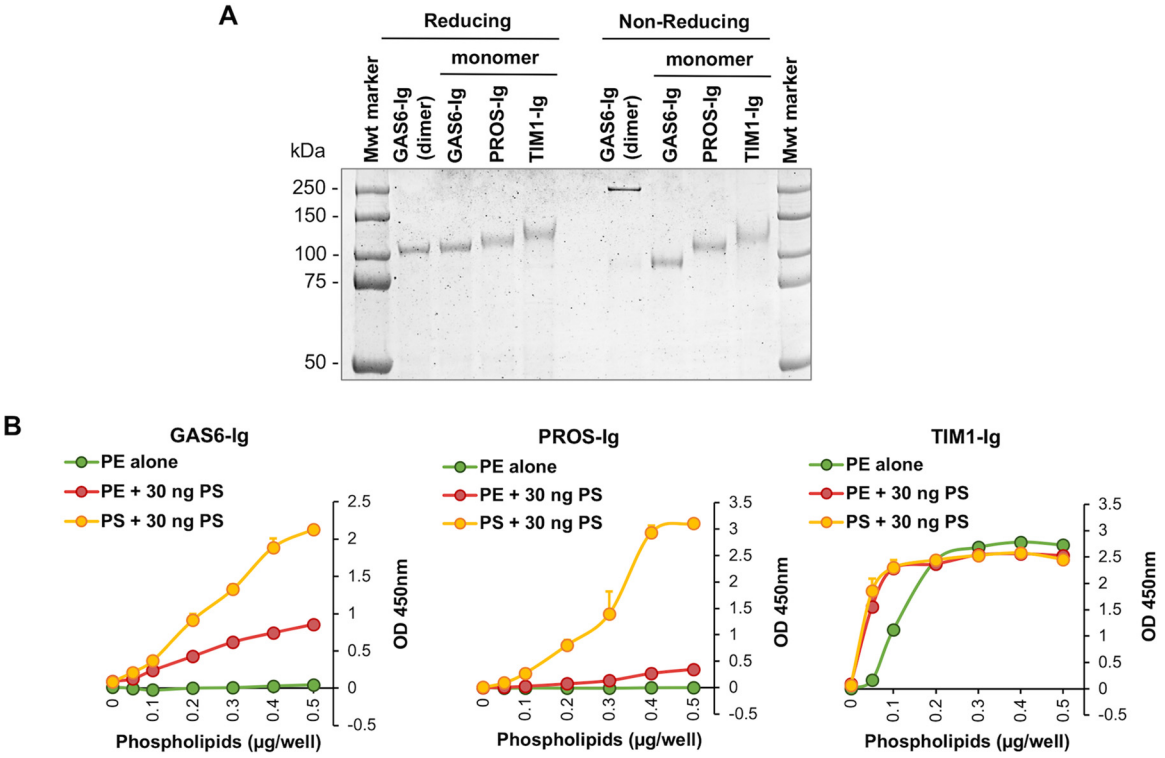

FIG A1 PS binding to GAS6, PROS, or TIM1 is enhanced by PE present on the same surface. (A) Monomeric Ig-fusion proteins used in ELISAs are analyzed by reducing and nonreducing SDS-PAGE. Dimeric GAS6-Ig is used as a control. (B) An increasing amount of PE or PS (0 to 0.5 μg per well) mixed with 30 ng of PS per well or an increasing amount of PE without PS was dried on the plates. Plates were incubated with 5 nM GAS6-Ig, PROS-Ig, or TIM1-Ig, and bound molecules were detected with an anti-human IgG antibody conjugated with HRP. Representatives of three similar experiments are shown.

ACKNOWLEDGMENT

This work was supported by the National Institutes of Health (R01 AI110692). The funders had no role in study design, data collection and interpretation, or the decision to submit the work for publication.

REFERENCES

1. Leventis PA, Grinstein S. 2010. The distribution and function of phosphatidylserine in cellular membranes. Annu Rev Biophys 39:407–427. https://doi.org/10.1146/annurev.biophys.093008.131234.
2. Amara A, Mercer J. 2015. Viral apoptotic mimicry. Nat Rev Microbiol 13:461–469. https://doi.org/10.1038/nrmicro3469.
3. Chua BA, Ngo JA, Situ K, Morizono K. 2019. Roles of phosphatidylserine exposed on the viral envelope and cell membrane in HIV-1 replication. Cell Commun Signal 17:132. https://doi.org/10.1186/s12964-019-0452-1.
4. Freeman GJ, Casasnovas JM, Umetsu DT, DeKruyff RH. 2010. TIM genes: a family of cell surface phosphatidylserine receptors that regulate innate and adaptive immunity. Immunol Rev 235:172–189. https://doi.org/10.1111/j.0105-2896.2010.00903.x.
5. Lemke G, Rothlin CV. 2008. Immunobiology of the TAM receptors. Nat Rev Immunol 8:327–336. https://doi.org/10.1038/nri2303.
6. Moller-Tank S, Maury W. 2014. Phosphatidylserine receptors: enhancers of enveloped virus entry and infection. Virology 468–470:565–580. https://doi.org/10.1016/j.virol.2014.09.009.
7. Morizono K, Chen IS. 2014. Role of phosphatidylserine receptors in enveloped virus infection. J Virol 88:4275–4290. https://doi.org/10.1128/JVI.03287-13.
8. Kuchroo VK, Meyers JH, Umetsu DT, DeKruyff RH. 2006. TIM family of genes in immunity and tolerance. Adv Immunol 91:227–249. https://doi.org/10.1016/S0065-2776(06)91006-2.
9. Evans JP, Liu SL. 2020. Multifaceted roles of TIM-family proteins in virus-host interactions. Trends Microbiol 28:224–235. https://doi.org/10.1016/j.tim.2019.10.004.
10. Ichimura T, Asseldonk EJ, Humphreys BD, Gunaratnam L, Duffield JS, Bonventre JV. 2008. Kidney injury molecule-1 is a phosphatidylserine receptor that confers a phagocytic phenotype on epithelial cells. J Clin Invest 118:1657–1668. https://doi.org/10.1172/JCI34487.
11. Stitt TN, Conn G, Gore M, Lai C, Bruno J, Radziejewski C, Mattsson K, Fisher J, Gies DR, Jones PF. 1995. The anticoagulation factor protein S and its relative, Gas6, are ligands for the Tyro 3/Axl family of receptor tyrosine kinases. Cell 80:661–670. https://doi.org/10.1016/0092-8674(95)90520-0.
12. Nagata K, Ohashi K, Nakano T, Arita H, Zong C, Hanafusa H, Mizuno K. 1996. Identification of the product of growth arrest-specific gene 6 as a common ligand for Axl, Sky, and Mer receptor tyrosine kinases. J Biol Chem 271:30022–30027. https://doi.org/10.1074/jbc.271.47.30022.
13. Varnum BC, Young C, Elliott G, Garcia A, Bartley TD, Fridell YW, Hunt RW, Trail G, Clogston C, Toso RJ, Yanagihara D, Bennett L, Sylber M, Merewether LA, Tseng A, Escobar E, Liu ET, Yamane HK. 1995. Axl receptor tyrosine kinase stimulated by the vitamin K-dependent protein encoded by growth-arrest-specific gene 6. Nature 373:623–626. https://doi.org/10.1038/373623a0.
14. Hafizi S, Dahlback B. 2006. Gas6 and protein S. Vitamin K-dependent ligands for the Axl receptor tyrosine kinase subfamily. FEBS J 273:5231–5244. https://doi.org/10.1111/j.1742-4658.2006.05529.x.
15. Godowski PJ, Mark MR, Chen J, Sadick MD, Raab H, Hammonds RG. 1995.

Reevaluation of the roles of protein S and Gas6 as ligands for the receptor tyrosine kinase Rse/Tyro3. Cell 82:355–358. https://doi.org/10.1016/0092-8674(95)90424-7.
16. Hall MO, Obin MS, Heeb MJ, Burgess BL, Abrams TA. 2005. Both protein S and Gas6 stimulate outer segment phagocytosis by cultured rat retinal pigment epithelial cells. Exp Eye Res 81:581–591. https://doi.org/10.1016/j.exer.2005.03.017.
17. Dahlback B, Lundwall A, Stenflo J. 1986. Primary structure of bovine vitamin K-dependent protein S. Proc Natl Acad Sci U S A 83:4199–4203. https://doi.org/10.1073/pnas.83.12.4199.
18. Murate M, Abe M, Kasahara K, Iwabuchi K, Umeda M, Kobayashi T. 2015. Transbilayer distribution of lipids at nano scale. J Cell Sci 128:1627–1638. https://doi.org/10.1242/jcs.163105.
19. Emoto K, Toyama-Sorimachi N, Karasuyama H, Inoue K, Umeda M. 1997. Exposure of phosphatidylethanolamine on the surface of apoptotic cells. Exp Cell Res 232:430–434. https://doi.org/10.1006/excr.1997.3521.
20. Richard AS, Zhang A, Park SJ, Farzan M, Zong M, Choe H. 2015. Virion-associated phosphatidylethanolamine promotes TIM1-mediated infection by Ebola, dengue, and West Nile viruses. Proc Natl Acad Sci U S A 112:14682–14687. https://doi.org/10.1073/pnas.1508095112.
21. Stafford JH, Thorpe PE. 2011. Increased exposure of phosphatidylethanolamine on the surface of tumor vascular endothelium. Neoplasia 13:299–308. https://doi.org/10.1593/neo.101366.
22. Carnec X, Meertens L, Dejarnac O, Perera-Lecoin M, Hafirassou ML, Kitaura J, Ramdasi R, Schwartz O, Amara A. 2016. The phosphatidylserine and phosphatidylethanolamine receptor CD300a binds dengue virus and enhances infection. J Virol 90:92–102. https://doi.org/10.1128/JVI.01849-15.
23. Neuenschwander PF, Bianco-Fisher E, Rezaie AR, Morrissey JH. 1995. Phosphatidylethanolamine augments factor VIIa-tissue factor activity: enhancement of sensitivity to phosphatidylserine. Biochemistry 34:13988–13993. https://doi.org/10.1021/bi00043a004.
24. Gilbert GE, Arena AA. 1995. Phosphatidylethanolamine induces high affinity binding sites for factor VIII on membranes containing phosphatidyl-L-serine. J Biol Chem 270:18500–18505. https://doi.org/10.1074/jbc.270.31.18500.
25. Tavoosi N, Davis-Harrison RL, Pogorelov TV, Ohkubo YZ, Arcario MJ, Clay MC, Rienstra CM, Tajkhorshid E, Morrissey JH. 2011. Molecular determinants of phospholipid synergy in blood clotting. J Biol Chem 286:23247–23253. https://doi.org/10.1074/jbc.M111.251769.
26. Majumder R, Liang X, Quinn-Allen MA, Kane WH, Lentz BR. 2011. Modulation of prothrombinase assembly and activity by phosphatidylethanolamine. J Biol Chem 286:35535–35542. https://doi.org/10.1074/jbc.M111.260141.
27. Nelsestuen GL, Broderius M. 1977. Interaction of prothrombin and blood-clotting factor X with membranes of varying composition. Biochemistry 16:4172–4177. https://doi.org/10.1021/bi00638a006.
28. Jain SK. 1985. In vivo externalization of phosphatidylserine and phosphatidylethanolamine in the membrane bilayer and hypercoagulability by the lipid peroxidation of erythrocytes in rats. J Clin Invest 76:281–286. https://doi.org/10.1172/JCI111958.
29. Manfioletti G, Brancolini C, Avanzi G, Schneider C. 1993. The protein encoded by a growth arrest-specific gene (gas6) is a new member of the vitamin K-dependent proteins related to protein S, a negative coregulator in the blood coagulation cascade. Mol Cell Biol 13:4976–4985. https://doi.org/10.1128/mcb.13.8.4976.
30. Nakano T, Higashino K, Kikuchi N, Kishino J, Nomura K, Fujita H, Ohara O, Arita H. 1995. Vascular smooth muscle cell-derived, Gla-containing growth-potentiating factor for Ca(2+)-mobilizing growth factors. J Biol Chem 270:5702–5705. https://doi.org/10.1074/jbc.270.11.5702.
31. Balogh I, Hafizi S, Stenhoff J, Hansson K, Dahlback B. 2005. Analysis of Gas6 in human platelets and plasma. Arterioscler Thromb Vasc Biol 25:1280–1286. https://doi.org/10.1161/01.ATV.0000163845.07146.48.
32. Griffin JH, Gruber A, Fernandez JA. 1992. Reevaluation of total, free, and bound protein S and C4b-binding protein levels in plasma anticoagulated with citrate or hirudin. Blood 79:3203–3211. https://doi.org/10.1182/blood.V79.12.3203.3203.
33. Blostein MD, Rajotte I, Rao DP, Holcroft CA, Kahn SR. 2011. Elevated plasma gas6 levels are associated with venous thromboembolic disease. J Thromb Thrombolysis 32:272–278. https://doi.org/10.1007/s11239-011-0597-2.
34. Jemielity S, Wang JJ, Chan YK, Ahmed AA, Li W, Monahan S, Bu X, Farzan M, Freeman GJ, Umetsu DT, Dekruyff RH, Choe H. 2013. TIM-family proteins promote infection of multiple enveloped viruses through virion-associated phosphatidylserine. PLoS Pathog 9:e1003232. https://doi.org/10.1371/journal.ppat.1003232.
35. Kondratowicz AS, Lennemann NJ, Sinn PL, Davey RA, Hunt CL, Moller-Tank S, Meyerholz DK, Rennert P, Mullins RF, Brindley M, Sandersfeld LM, Quinn K, Weller M, McCray PB, Jr, Chiorini J, Maury W. 2011. T-cell immunoglobulin and mucin domain 1 (TIM-1) is a receptor for Zaire Ebolavirus and Lake Victoria Marburgvirus. Proc Natl Acad Sci U S A 108:8426–8431. https://doi.org/10.1073/pnas.1019030108.
36. Meertens L, Carnec X, Lecoin MP, Ramdasi R, Guivel-Benhassine F, Lew E, Lemke G, Schwartz O, Amara A. 2012. The TIM and TAM families of phosphatidylserine receptors mediate dengue virus entry. Cell Host Microbe 12:544–557. https://doi.org/10.1016/j.chom.2012.08.009.
37. Morizono K, Xie Y, Olafsen T, Lee B, Dasgupta A, Wu AM, Chen IS. 2011. The soluble serum protein Gas6 bridges virion envelope phosphatidylserine to the TAM receptor tyrosine kinase Axl to mediate viral entry. Cell Host Microbe 9:286–298. https://doi.org/10.1016/j.chom.2011.03.012.
38. Soares MM, King SW, Thorpe PE. 2008. Targeting inside-out phosphatidylserine as a therapeutic strategy for viral diseases. Nat Med 14:1357–1362. https://doi.org/10.1038/nm.1885.
39. Meertens L, Labeau A, Dejarnac O, Cipriani S, Sinigaglia L, Bonnet-Madin L, Le Charpentier T, Hafirassou ML, Zamborlini A, Cao-Lormeau VM, Coulpier M, Misse D, Jouvenet N, Tabibiazar R, Gressens P, Schwartz O, Amara A. 2017. Axl mediates ZIKA virus entry in human glial cells and modulates innate immune responses. Cell Rep 18:324–333. https://doi.org/10.1016/j.celrep.2016.12.045.
40. Richard AS, Shim BS, Kwon YC, Zhang R, Otsuka Y, Schmitt K, Berri F, Diamond MS, Choe H. 2017. AXL-dependent infection of human fetal endothelial cells distinguishes Zika virus from other pathogenic flaviviruses. Proc Natl Acad Sci U S A 114:2024–2029. https://doi.org/10.1073/pnas.1620558114.
41. Mercer J, Helenius A. 2008. Vaccinia virus uses macropinocytosis and apoptotic mimicry to enter host cells. Science 320:531–535. https://doi.org/10.1126/science.1155164.
42. Shimojima M, Stroher U, Ebihara H, Feldmann H, Kawaoka Y. 2012. Identification of cell surface molecules involved in dystroglycan-independent Lassa virus cell entry. J Virol 86:2067–2078. https://doi.org/10.1128/JVI.06451-11.
43. Hamel R, Dejarnac O, Wichit S, Ekchariyawat P, Neyret A, Luplertlop N, Perera-Lecoin M, Surasombatpattana P, Talignani L, Thomas F, Cao-Lormeau VM, Choumet V, Briant L, Despres P, Amara A, Yssel H, Misse D. 2015. Biology of Zika virus infection in human skin cells. J Virol 89:8880–8896. https://doi.org/10.1128/JVI.00354-15.
44. Brindley MA, Hunt CL, Kondratowicz AS, Bowman J, Sinn PL, McCray PB, Jr, Quinn K, Weller ML, Chiorini JA, Maury W. 2011. Tyrosine kinase receptor Axl enhances entry of Zaire ebolavirus without direct interactions with the viral glycoprotein. Virology 415:83–94. https://doi.org/10.1016/j.virol.2011.04.002.
45. Liu S, DeLalio LJ, Isakson BE, Wang TT. 2016. AXL-mediated productive infection of human endothelial cells by Zika virus. Circ Res 119:1183–1189. https://doi.org/10.1161/CIRCRESAHA.116.309866.
46. Brouillette RB, Phillips EK, Patel R, Mahauad-Fernandez W, Moller-Tank S, Rogers KJ, Dillard JA, Cooney AL, Martinez-Sobrido L, Okeoma C, Maury W. 2018. TIM-1 mediates dystroglycan-independent entry of Lassa virus. J Virol 92:e00093-18. https://doi.org/10.1128/JVI.00093-18.
47. Fast PG. 1966. A comparative study of the phospholipids and fatty acids of some insects. Lipids 1:209–215. https://doi.org/10.1007/BF02531874.